Fading Reduction by Aperture Averaging and Spatial Diversity in Optical Wireless Systems

Mohammad-Ali Khalighi, Noah Schwartz, Naziha Aitamer, and Salah Bourennane

***Abstract*—Atmospheric turbulence can cause a significant performance degradation in free-space optical communication systems. It is well known that the effect of turbulence can be reduced by performing aperture averaging and/or employing spatial diversity at the receiver. In this paper, we provide a synthesis on the effectiveness of these techniques under different atmospheric turbulence conditions from a telecommunication point of view. In particular, we quantify the performance improvement in terms of average bit error rate (BER) and outage capacity, which are among important parameters in practice. The efficiency of channel coding and the feasibility of exploiting time diversity in aperture averaging receivers are discussed as well. We also compare single- and multiple-aperture systems from the point of view of fading reduction by considering uncorrelated fading on adjacent apertures for the latter case. We show that when the receiver is background noise limited, the use of multiple apertures is largely preferred to a single large aperture under strong turbulence conditions. A single aperture is likely to be preferred under moderate turbulence conditions, however. When the receiver is thermal noise limited, even under strong turbulence conditions, the use of multiple apertures is interesting only when working at a very low BER. We also provide discussions on several practical issues related to system implementation.**

***Index Terms*—Atmospheric turbulence; Aperture averaging; Spatial diversity; Free-space optics**.

I. Introduction

Free-space optical (FSO) communication systems can provide huge data transmission rates and have attracted considerable attention during the past few years for a variety of applications and markets [1–3]. In practice, considering clear sky conditions, atmospheric turbulence causes random fluctuations of the phase and the amplitude of the received signal, or in other words, channel *fading*. These intensity fluctuations, called scintillation, can result in a considerable degradation of the system performance. Fading is more significant in long-distance transmissions as well as in the case of communication with a moving platform. A comprehensive survey of optical-propagation effects can be found in [4].

It is well known that to mitigate efficiently channel fading, one can make use of diversity techniques. We have considered in previous work [5,6] the use of time diversity and shown that substantial performance improvement can be obtained by performing channel coding and interleaving. Another approach proposed in [7] considers the transmission of the data stream twice, on two polarizations, for example, with enough delay between them; data detection at the receiver is then done based on the two streams. A generalization of this scheme is considered in [8] as well. All these approaches, however, often impose long delay latencies and necessitate the use of large memories for storing long data frames. Another solution is to employ spatial diversity for fading reduction. Aperture averaging can be seen as a simple form of spatial diversity when the receiver lens aperture is larger than the fading correlation length [4,9]. The use of aperture averaging for reducing the effect of scintillation has been widely considered in the literature and in practical systems [4,9–17]. Fading reduction is usually quantified by considering the so-called aperture averaging factor (defined later in Subsection III.B). It is shown that substantial scintillation reduction can be obtained, especially in the case of strong turbulence. Better scintillation reduction could be obtained by using multiple lenses at the receiver and/or using multiple beams at the transmitter [8,18].

Here, we consider the case where we work with a monochromatic laser and a single beam at the transmitter. Our aim is to study the impact of aperture averaging on the system performance by considering as

Manuscript received June 19, 2009; revised September 25, 2009; accepted October 9, 2009; published October 30, 2009 (Doc. ID 113009).

M.-A. Khalighi (e-mail: Ali.Khalighi@fresnel.fr), N. Aitamer, and S. Bourennane are with École Centrale Marseille, Institut Fresnel, UMR CNRS 6133, Marseille, France.

N. Schwartz is with the Department of Theoretical and Applied Optics (DOTA), ONERA, Châtillon, France.

Digital Object Identifier 10.1364/JOCN.1.000580

criteria the system average bit error rate (BER) as well as the outage capacity C_{out}, which are important parameters in a practical FSO system because they are directly related to the quality of data transmission and link availability. Through realistic examples and case studies we show the effective performance improvement under different turbulence conditions. First, we review aperture averaging receivers and show the performance gain for different turbulence regimes by presenting some numerical results. In particular, we illustrate the impact of the inner scale of turbulence. The efficiency of channel coding in reducing the system BER is also studied. Then, we consider multiple aperture receivers, assuming uncorrelated fading on adjacent apertures, and compare their performances with that of a single aperture receiver of the same overall aperture size. In contrast to the previous works such as [4,8], we will discuss the rationality of preferring one solution to another for different practical aperture sizes. In particular, we consider two cases of background and thermal noise-limited receivers. We show that for the former case, the use of multiple apertures is largely preferred to that of a single large aperture under strong turbulence conditions. A single aperture is likely to be preferred under moderate turbulence conditions, however. For the latter case, we show that, even under strong turbulence conditions, the use of multiple apertures is interesting only when working at very low BER.

Note that numerous works have already appeared on this topic. Yet, our motivation behind this work has been to quantify the the system performance in terms of BER and C_{out} and to evaluate the improvement by considering these parameters. This would make more sense for people from the telecommunication and signal processing community who are not necessarily familiar with the physical phenomena behind optical wave propagation. Meanwhile, we make the analogy with the classical aperture averaging factor criterion that is usually considered in the literature. The parameters considered in our synthesis such as receiver aperture sizes are rational and mostly correspond to those used in practical FSO systems. In view of providing perspectives to design engineers, in addition to the *theoretical* studies, we also provide discussions on the implementation issues and the corresponding limitations on the performance improvement. In particular, we consider the impact of channel coding and signal modulation, the feasibility of exploiting time diversity, the limitation or not of the aperture averaging gain by the detector size, and the feasibility of attaining uncorrelated fading conditions for multiple aperture receivers. To the best of our knowledge, such a synthesis that brings all these points together is missing in the literature.

The organization of the paper is as follows. In Section II, we present the main assumptions concerning signal transmission and detection. In Section III, we provide some generalities on turbulence modeling. We present some numerical results in Section IV to study the performance improvement by aperture averaging by considering the aperture averaging factor and the average BER. Then, the impact of channel coding used in combination with aperture averaging is studied in Section V. Next, we consider the improvement in terms of the outage capacity in Section VI. A comparison of single- and multiple-aperture receivers is then presented in Section VII. Finally, Section VIII concludes the paper.

II. System Model and Assumptions

Consider a typical FSO system, where the information-bearing laser beam is projected onto the optical receiver along the line of sight. For the sake of implementation simplicity, we consider intensity modulation with direct detection (IM/DD) because it is used in most current optical communication systems. At the transmitter, binary data are converted to impulses of duration T_s according to the nonreturn-to-zero (NRZ) on–off keying (OOK) modulation, unless otherwise specified. At the receiver, the incident beam is collected on a lens of diameter D before being focused on a photodetector that converts it to an electrical signal. We present the system model based on the received signal intensity and not on photon counting, as sometimes considered in the literature [19]. The latter is essentially adapted to deep-space FSO systems. In fact, in most terrestrial FSO systems, the received flux is important enough to allow working with the beam intensity directly. In addition, photon counting could not be done practically. Let the received signal be

$$r = \eta I + n, \tag{1}$$

where η is the optical/electrical conversion efficiency. Also, n is the sum of thermal, dark, background, and shot noise and is modeled as a Gaussian white stationary random process of variance σ_n^2. The Gaussian assumption is usually used for thermal and background noise. In shot-noise-limited receivers, the Gaussian assumption could still be used, but the noise power will depend on the received signal intensity; that is, it will depend on whether a one or a zero is transmitted [20]. We assume that the shot-noise contribution in n is negligible.

Without loss of generality, we set $\eta = 1$. After optical/electrical conversion and sampling, we perform signal demodulation. In this work, we consider optimal signal detection at the receiver based on the maximum *a posteriori* (MAP) criterion, assuming perfect channel knowledge. Note that the channel can be estimated

based on some training symbols [21], and the results are very close to the perfect channel knowledge case by using only a few pilots [5]. In the results to be presented, we will not consider any channel coding, unless otherwise mentioned. We consider the quasi-static channel model by which the channel fading coefficients remain constant during the transmission of a frame of symbols. We will later explain in Section V the rationality of this assumption.

To compare the receiver performance for different lens diameters D, we fix the noise variance σ_n^2 and also consider normalized average received intensity, i.e., we set $E\{I\}=1$. This, in fact, represents a background-noise-limited fixed field-of-view (FOV) receiver. In such a case, by increasing the pupil area by a factor m, the received signal and noise powers increase by the same factor [22], and hence, the signal-to-noise ratio (SNR) does not change. Note that this is valid when either optical or electrical SNR is considered. If the receiver is thermal noise limited, the noise variance does not depend on D, but by setting $E\{I\}$ to 1, we will not take into account the gain in the signal power. Nevertheless, the comparison of different systems in this way remains interesting because it helps to investigate the improvement in terms of fading reduction.

Finally, we assume that the photodetector area is sufficiently large to permit the system to benefit fully from aperture averaging, irrespective of the turbulence strength (discussions on this assumption are made in Section VIII). Other assumptions on the atmospheric turbulence will be specified later in Subsection IV.A after presenting the turbulence modeling. Let us summarize our main assumptions before proceeding to the next section:

- Channel time variations are very slow; the quasi-static model applies.
- The normalized SNR is considered at the receiver for any aperture size.
- The photodetector area is sufficiently large to collect the whole optical beam at the focal plane of the receiver.

III. Turbulence Modeling

A comprehensive study of turbulence modeling can be found in [4]. Atmospheric turbulence can be characterized by three parameters: the inner scale l_0, the outer scale L_0, and the index of the refraction structure parameter C_n^2, sometimes called the turbulence strength [23]. Throughout the paper, we consider the context of terrestrial FSO systems and assume the condition of homogeneous turbulence. That is, we assume that C_n^2 does not depend on the distance. Generally, the distinction between different turbulence regimes is made based on the Rytov variance σ_R^2:

$$\sigma_R^2 = 1.23 C_n^2 k^{7/6} L^{11/6}, \tag{2}$$

where $k=2\pi/\lambda$ is the wave number with λ being the wavelength, and L is the link distance. In this way, weak, moderate, and strong turbulence conditions are characterized by $\sigma_R^2<1$, $\sigma_R^2\approx 1$, and $\sigma_R^2\gg 1$, respectively. Notice that σ_R^2 is just a theoretical parameter that is used for specifying the turbulence conditions. In the weak turbulence regime, we have $\sigma_R^2\approx\sigma_{\ln I}^2\approx\sigma_I^2$, where $\sigma_{\ln I}^2$ and σ_I^2 denote the variance of log intensity fluctuations and the scintillation index, respectively. For relatively strong turbulence conditions, we enter the saturation regime, and the scintillation index can be much smaller than that predicted by the Rytov model. Let us recall some definitions that we will use later in the paper:

- Fresnel zone $F=\sqrt{L/k}$;
- coherence radius $\rho_0=(1.46C_n^2k^2L)^{-3/5}$, $l_0\ll\rho_0\ll L_0$ (expression valid for the plane-wave propagation model [4]);
- scattering disk $L/k\rho_0$.

Note that under moderate to strong turbulence conditions, only eddies smaller than ρ_0 or larger than the scattering disk $L/k\rho_0$ contribute effectively to the atmospheric turbulence [4].

A. Propagation Model

In the literature, usually the plane- or spherical-wave propagation models are considered. These models that are simpler and more analytically tractable hold with the approximation of a point optical source. Sometimes, analyses are done assuming a collimated Gaussian-beam wave, where the power profile of the beam is close to a Gaussian. For optical links through space, the plane-wave propagation model is mostly appropriate for space-to-ground transmissions, whereas the spherical propagation model is suitable for ground-to-space transmission links. For horizontal (terrestrial) transmissions, the Gaussian-beam model is a good approximation, however [24]. It should be noted that, when the Gaussian beam has a relatively large divergence, its statistical properties are close to the case of a point source [12]. For such a beam, we can effectively use the approximations of plane or spherical waves. Unless otherwise mentioned, for the sake of modeling simplicity, we consider in this paper the conditions of plane-wave propagation.

B. Statistical Modeling

For intensity fluctuations, we adopt the Gamma–Gamma ($\Gamma\Gamma$) channel model that can describe any type of turbulence, i.e., weak, moderate, or strong. The corresponding probability density function (PDF) is

$$P(I) = \frac{2(\alpha\beta)^{(\alpha+\beta)/2}}{\Gamma(\alpha)\Gamma(\beta)} I^{(\alpha+\beta)/2-1} K_{\alpha-\beta}[2(\alpha\beta I)^{1/2}], \quad I > 0, \tag{3}$$

where α and β are effective numbers of large- and small-scale eddies of the scattering environment, respectively, and are directly related to the atmospheric conditions. Also, $K_\alpha(x)$ is the modified Bessel function of the second kind and order α. Expressions for calculating the parameters α and β for different propagation conditions can be found in [4].

Let us denote by $\sigma_I^2(D)$ the scintillation index, i.e., the variance of intensity fluctuations, for a receiver lens of diameter D. The effect of aperture averaging is to decrease this variance for $D>0$. The $\Gamma\Gamma$ statistical model can still be used with modified parameters α and β. For a given D, the effectiveness of aperture averaging depends on the propagation conditions. Here, we just recall the expression of σ_I^2 for the case of plane-wave propagation, $L_0 \approx \infty$, and $l_0 \approx 0$ [4]:

$$\sigma_{I,\mathrm{PL}}^2(D) = \exp\left[\frac{0.49\sigma_R^2}{(1+0.653d^2+1.11\sigma_R^{12/5})^{7/6}} + \frac{0.51\sigma_R^2(1+0.69\sigma_R^{12/5})^{-5/6}}{1+0.9d^2+0.621d^2\sigma_R^{12/5}} \right] - 1, \tag{4}$$

where $d=\sqrt{kD^2/4L}$ is the circular aperture radius scaled by the Fresnel zone, and the subscript PL denotes explicitly the assumption of plane-wave propagation. The parameter that is usually used to quantify the fading reduction by aperture averaging is the aperture averaging factor:

$$A = \frac{\sigma_I^2(D)}{\sigma_I^2(0)}, \tag{5}$$

where $\sigma_I^2(0)$ denotes the scintillation index for a *point receiver* ($D=0$). For the weak fluctuation regime, A can be approximated as [4]

$$A \approx \left[1 + 1.062\left(\frac{D^2}{4}\frac{k}{L}\right) \right]^{-7/6}. \tag{6}$$

IV. Effect of Aperture Averaging

We present here some simulation results to study the effect of aperture averaging under different turbulence conditions.

A. Parameters Considered for Numerical Results

We consider a wavelength of $\lambda=1550$ nm. Three cases of strong, moderate, and weak turbulence are considered, for which we set $L=1500$ m and $C_n^2=4.58\times10^{-13}$ m$^{-2/3}$, $L=500$ m and $C_n^2=4.58\times10^{-13}$ m$^{-2/3}$, and $L=500$ m and $C_n^2=7\times10^{-16}$ m$^{-2/3}$, respectively. Using Eq. (2), the Rytov variance corresponding to these three cases is $\sigma_R^2=19.18$, $\sigma_R^2=2.56$, and $\sigma_R^2=0.004$, respectively. The inner scale is set to $l_0=4.6$ mm, based on the experimental results of [9] for $C_n^2=4.58\times10^{-13}$ and $\lambda=1550$ nm. We neglect the outer scale as it has a negligible impact on the scintillation index in practice [4]; i.e., we assume that $L_0\approx\infty$.

For the simulations, we will present the receiver performance in terms of average BER as a function of SNR. We consider the electrical SNR in the form of E_b/N_0, where E_b is the average received energy per information bit, and N_0 is the unilateral noise power spectral density. For the case of uncoded OOK, E_b/N_0 equals the actual SNR. At the receiver, the electrical signal power is considered as $E\{I^2\}$. For temporal variations of the turbulence, we use the quasi-static (frozen) channel model. Each frame corresponds to 2000 bits. Since a quasi-static channel is considered, the frame length has almost no impact on the BER results to be presented.

B. Aperture Averaging Factor

The aperture averaging factor A has already been studied in numerous works. Nevertheless, we prefer to briefly recall the general points by considering the three special cases of weak, moderate, and strong turbulence, specified above. These results are useful when discussing other simulation results presented later in this section. For the classical case of plane-wave propagation, we have presented the curves of A versus the normalized receiver lens radius d in Fig. 1. For the moderate and strong turbulence regimes, both cases of $l_0=0$ and $l_0=4.6$ mm are considered.

For $l_0=0$, we have almost the same behavior for the weak and moderate turbulence cases. For the strong turbulence regime, we have the famous leveling effect predicted for $\rho_0<D<L/k\rho_0$; A continues to decrease for $D>L/k\rho_0$ [13]. From Fig. 1, the leveling effect can be attributed to about $1<d<5$, or equivalently to

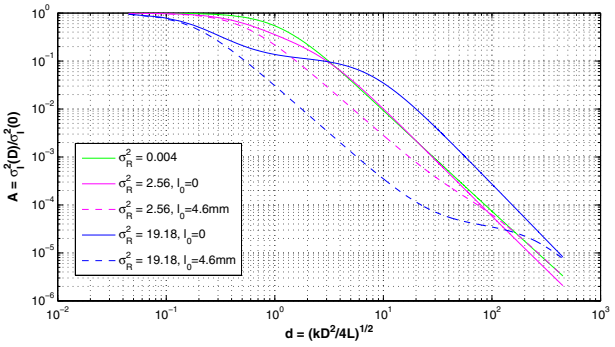

Fig. 1. (Color online) Aperture averaging factor, plane-wave propagation.

38 mm $< D <$ 150 mm. Remembering the parameters from Subsection IV.A, for this case, we have $\rho_0 = 3$ mm and $L/k\rho_0 = 123$ mm.

We propose here an interpretation for the results of Fig. 1, notably concerning the leveling effect, by considering the scintillation speckles at the receiver. For weak to moderate turbulence regimes, the scintillation speckles at the receiver have roughly a circular shape with the size of the order of $\sqrt{\lambda L}$ [25]. For these cases, we see that A begins to decrease effectively for $D > \sqrt{\lambda L}$ because the pupil can effectively average over an increasing number of speckles. For the cases of relatively strong turbulence, the scintillation speckles at the receiver have an elongated shape with two characteristic sizes $d_1 = r_0$ and $d_2 = \lambda L/r_0$, where r_0 is the Fried parameter [26]. By increasing D, we first average over the d_1 dimension where A decreases steadily. Then, we reach the area of the leveling effect where we cannot average effectively over d_2 (while continuing to average over d_1) until D is increased sufficiently. To better understand this point, we have presented the intensity fluctuation spatial spectrum for the case of weak and strong turbulence in Fig. 2.

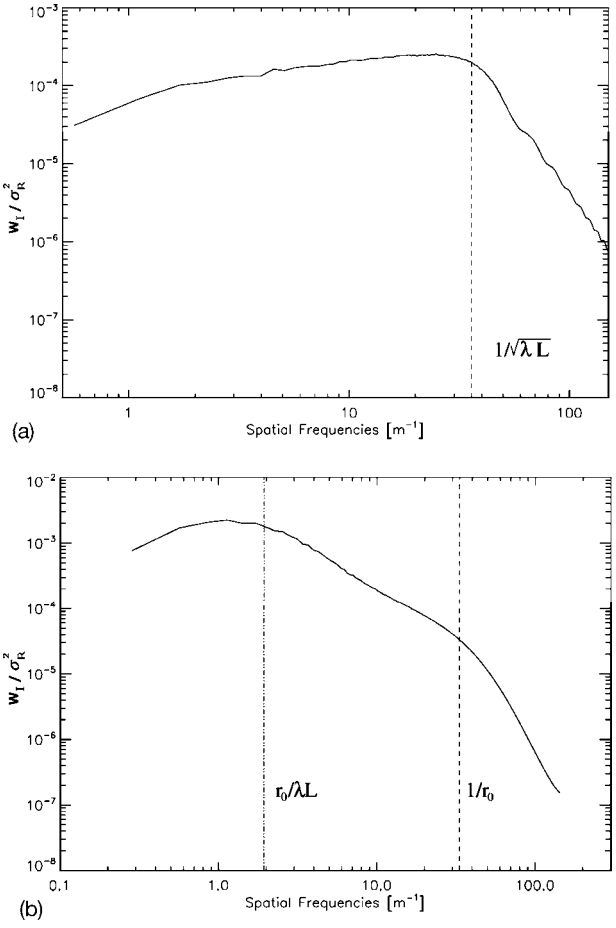

Fig. 2. Spatial spectrum W_I of intensity fluctuations normalized by the Rytov variance σ_R^2 for (a) weak turbulence regime and (b) strong turbulence regime. Spectra are obtained via simulating wave propagation through turbulence using the phase screens method.

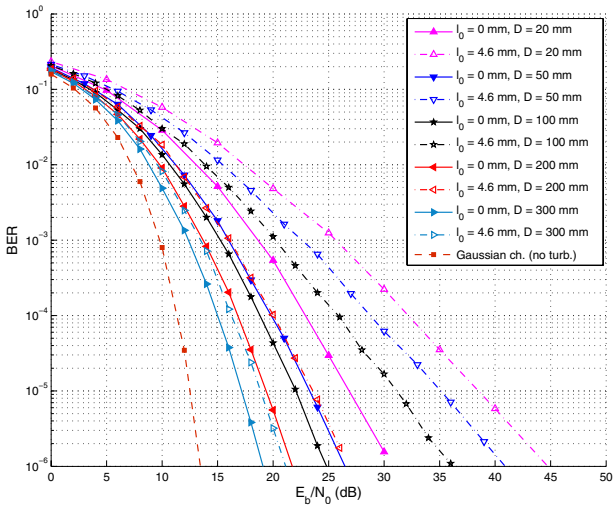

Fig. 3. (Color online) Average BER performance in the strong turbulence regime with $\sigma_R^2 = 19.18$, plane-wave propagation.

If the inner scale l_0 is not negligible, we notice from Fig. 1 that the aperture averaging is more effective. This can be explained by the fact that larger inner scales result in larger values of irradiance variance, i.e., $\sigma_I^2(0)$ for the strong turbulence regime [27,28]. This is also seen in the case of moderate turbulence, but the difference is much less important. The slight shift in the leveling effect might be explained by a slight shift of characteristic frequencies of the spatial intensity spectrum for $l_0 \neq 0$ [28].

C. Average BER Performance

Let us now consider the average BER performance of the receiver. We begin with the strong turbulence regime. BER curves for the case of plane-wave propagation are shown in Fig. 3 for $l_0 = 0$ and $l_0 = 4.6$ mm and different lens diameters D. We have also provided the corresponding curve for the Gaussian channel case, i.e., in the absence of turbulence, as a reference. Notice that in practical FSO systems, the guaranteed link BER is usually of the order of 10^{-9} or even lower. However, due to long Monte Carlo simulations, we have limited the results to BERs of about 10^{-6}. (For a given SNR, we generate as many frames as necessary to obtain at least 1000 frame errors and 5000 bit errors.) We have only presented the BER curves for somewhat practical values of D. To see the comparison with smaller D and especially with the case of a point receiver, see [29].

Let us first consider the case of $l_0 = 0$ for which we have $\rho_0 = 3$ mm and $L/k\rho_0 = 123$ mm. We notice from Fig. 3 that significant performance improvement is achieved by increasing the receiver aperture size. For instance, by increasing D from 20 to 100 mm, we obtain a gain of about 7 dB in SNR at the BER of 10^{-5}. From Fig. 1, saturation of A was predicted for

38 mm $< D <$ 150 mm. This is confirmed by the BER curves: We have a relatively small improvement by increasing D from 50 to 100 mm, but for $D \geq 200$ mm, we have again an effective decrease in BER.

When the inner scale of turbulence is not negligible, the turbulence has a more destructive effect [27]. Besides, as we see from Fig. 3 (dashed curves), we have a more significant decrease in BER for $l_0 = 4.6$ mm, even when increasing D from 200 to 300 mm, for example. This again confirms the results of Fig. 1. Note that, although for relatively large D ($D \geq 200$ mm), the performance for $l_0 = 4.6$ mm approaches that for $l_0 = 0$, there still remains a considerable difference between the corresponding BER curves.

Let us now consider the case of moderate turbulence. Results are shown in Fig. 4. Remembering the parameters from Subsection IV.A, for this case, we have $\rho_0 = 5.8$ mm and $L/k\rho_0 = 21$ mm. We notice that for $D > 50$ mm, the BER curves for $l_0 = 0$ are very close to the those for $l_0 \neq 0$. The fact that aperture averaging reduces the effect of l_0 is hence confirmed clearly. With $D = 300$ mm, we are very close to the case of the no-turbulence (Gaussian) channel.

Finally, Fig. 5 shows the BER curves for the weak turbulence regime. Here, "Pt Rx" denotes the case of a point receiver, i.e., the absence of aperture averaging. No surprise, the gain obtained by aperture averaging is far less impressive than that for moderate or strong turbulence regimes. For instance, for a BER of 10^{-5}, compared with the point receiver, we obtain only a gain of 0.33 dB in SNR, by using a 50 mm lens.

When more complex modulation techniques are used, the performance improvement by fading reduction via aperture averaging is more significant. As an example, for the case of a moderate turbulence regime, we have presented in Fig. 6 the SNR gain to achieve the BER of 10^{-5} for different lens diameters D when Q-ary pulse position modulation (PPM) [22] is used. The SNR gain is with respect to a point receiver, and three cases of $Q = 2$, 4, and 8 are considered. The performance of binary PPM (BPPM) is the same as that of OOK. We notice from Fig. 6 a larger gain for increased modulation order Q.

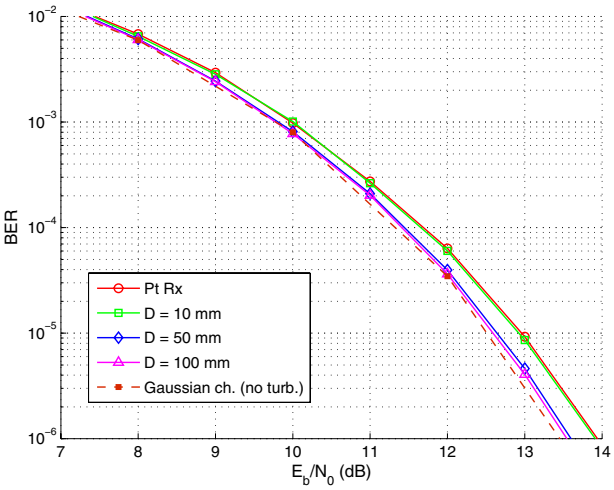

Fig. 5. (Color online) Average BER performance in the weak turbulence regime with $\sigma_R^2 = 0.004$, plane-wave propagation model. "Pt Rx" denotes the point receiver case ($D = 0$).

D. Effect of Propagation Model and Impact on Fade Statistics

Compared with the case of plane-wave propagation, the performance improvement by aperture averaging is less significant for the spherical-wave propagation case. It is the inverse round for the Gaussian-beam model where substantial improvement is obtained by aperture averaging. The reader is referred to [29] for some numerical results on the comparison of these cases. The interesting point is that, for large aperture

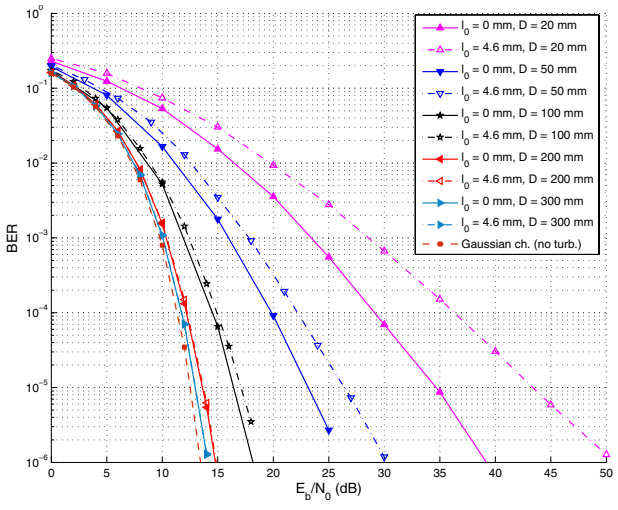

Fig. 4. (Color online) Average BER performance in the moderate turbulence regime with $\sigma_R^2 = 2.56$, plane-wave propagation.

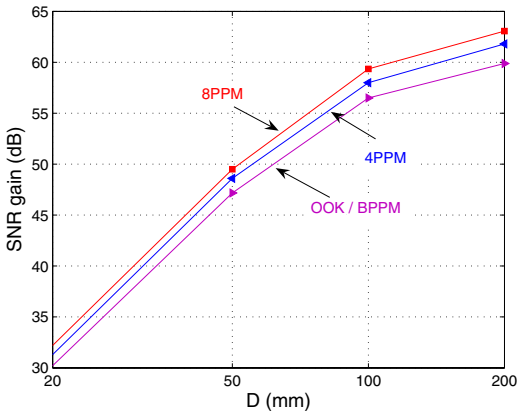

Fig. 6. (Color online) Gain in E_b/N_0 (with respect to a point receiver) versus receiver lens diameter D for BPPM, 4PPM, and 8PPM. Moderate turbulence regime with $\sigma_R^2 = 2.56$, plane-wave propagation, $l_0 = 4.6$ mm, BER $= 10^{-5}$.

sizes, as well as for the point receiver case, the BER curves of the Gaussian-beam model are close to those of the plane-wave model [29]. In such cases, we may adopt the approximation of plane-wave propagation for a Gaussian beam.

Concerning the fade statistics, since averaging is specially done over the small-scale fluctuations, the PDF of the channel fades shifts toward that of the large-scale fluctuations [30]. Experimental results show that the resulting scintillation after the receiver lens is better described by a log-normal (LN) distribution [7,9]. We have shown in [29] that the ΓΓ and LN models become practically equivalent for $D \gg \rho_0$ (roughly for $D > 6\rho_0$). We will make use of this property later in Section VI.

V. Effect of Channel Coding

Here, we investigate the effectiveness of channel coding for aperture averaging receivers assuming a quasi-static channel. We consider a simple rate 1/2 recursive systematic convolutional (RSC) code of constraint length $K=4$, with the octal representation (1,15/17). The reason we chose this code is that the classical convolutional codes have been shown to be a suitable choice for use in FSO systems under any turbulence regime because they make a good compromise between complexity and performance [5].

A. Coding Gain for Different Turbulence Regimes

We have shown in Fig. 7, the gain in E_b/N_0 required to obtain BER$=10^{-5}$, achieved by aperture averaging with and without RSC channel coding. The gain is with respect to the E_b/N_0 required for an uncoded system using a point receiver. (The point $D=1$ mm corresponds to a point receiver; we set this value in order to represent D in the logarithmic scale.). Note that arguing in terms of E_b/N_0 has the advantage of taking into account the channel coding rate, and thus, to make a fair comparison with the uncoded case.

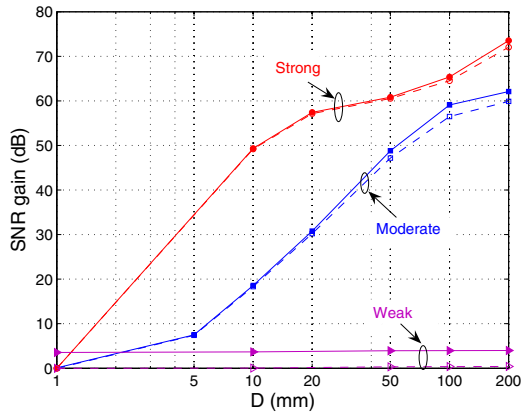

Fig. 7. (Color online) Gain in E_b/N_0 (with respect to a point receiver without coding) versus receiver lens diameter D for the three cases of turbulence, plane-wave propagation, $l_0=4.6$ mm, BER $=10^{-5}$. Dashed curves, aperture averaging without coding: solid curves, aperture averaging+RSC (1,15/17) coding.

From Fig. 7 we notice that we have a relatively significant gain for the case of weak turbulence, irrespective of D. For instance, for $D=50$ mm, we have an SNR gain of 3.6 dB. For the cases of moderate and strong turbulence, however, channel coding appears to be inefficient except for very large D. For instance, for $D=200$ mm, we have SNR gains of 2.2 and 1.6 dB for the moderate and strong turbulence cases, respectively.[1] There is negligible improvement in the SNR gain when employing more powerful codes (results are not shown). We conclude that channel coding is suitable only for the weak turbulence regime or when a large aperture size is used. In fact, as expected, coding is not efficient against fading. It becomes increasingly interesting only when we have a low fading channel or when the impact of turbulence can be significantly reduced, for example, by means of aperture averaging, spatial diversity, or adaptive optics.

B. Feasibility of Exploiting Time Diversity

When the aperture size is relatively small so that the aperture averaging benefit is poor, we can perform channel coding and interleaving over long enough frames (with respect to the channel coherence time τ_c) or use delayed copies of data streams in order to benefit from some time diversity [5,7,8]. When using a relatively large aperture size, however, exploiting time diversity becomes practically infeasible. In fact, assuming that the channel time variations are mostly due to the transversal wind (with respect to the optical axis), the use of a relatively large aperture size results in a large effective channel coherence time. Indeed, by this assumption and considering the Taylor hypothesis of frozen atmosphere, the spatial and temporal channel coordinates are related through the speed of the transversal wind $V_\perp$ [31]. The temporal evolution of the turbulence being due to $V_\perp$, by aperture averaging, we also average over the channel time variations. At the limit of $D \to \infty$, we have $\tau_c \to \infty$ too. Consequently, to benefit from time diversity, we have to use interleaver sizes that are too large or to introduce large delays between multiple transmissions of a data stream. This, in turn, imposes delay latencies that are too long and necessitates the use of huge memory sizes at the receiver. As a matter of fact, the Taylor hypothesis is somewhat pessimistic. In practice and for long transmission ranges, we have slightly shorter τ_c than that predicted by the Taylor model, due to turbulence *boiling*. Nevertheless, exploiting

[1]Meanwhile, we can see the leveling in the curve of SNR gain for the case of strong turbulence as explained in Subsection IV.B.

temporal diversity remains difficult from a practical point of view for relatively large D.

VI. Outage Capacity and the Impact of Aperture Averaging

Let us now study the impact of aperture averaging on the channel capacity. In most FSO systems subject to fading, we have a relatively slowly varying channel, and hence, the outage capacity (capacity versus outage) is an appropriate performance measurement criterion.

The channel capacity is defined as the maximum of the mutual information $\mathcal{I}(b;r)$ between the channel input and output, denoted here by b and r, respectively. The maximization is done over the input distribution $P_B(b)$:

$$C = \max_{P_B(b)} \mathcal{I}(b;r). \tag{7}$$

Here, we do not consider C in the sense of Shannon capacity; we impose the constraints of OOK modulation with equally likely symbols. The probability mass function of the input is $P_B(b)=1/2$, $b=0,1$. Imposing these constraints in Eq. (7) gives the the maximum transmission rate that we denote by C_{OOK}. Note that we have $\max(C_{\mathrm{OOK}})=1$ in units of bit per channel use. From Eq. (1), we have $r=bI+n$, where I is the received intensity. Conditioned to the received intensity I, C_{OOK} is given by

$$C_{\mathrm{OOK}} = \int_{-\infty}^{+\infty} \sum_{b=0,1} P_B(b) f_R(r) \log_2 \left(\frac{f_R(r|b)}{\sum_{b=0}^{1} P_B(b) f_R(r|b)} \right) \mathrm{d}r, \tag{8}$$

where r is Gaussian distributed of mean zero or I (depending on b) and of variance σ_n^2. After simplification, we obtain

$$C_{\mathrm{OOK}} = \frac{1}{2\sqrt{2\pi}} \int_{-\infty}^{+\infty} e^{-t^2/2} \log_2(1 + 2e^{-\theta^2/2} \sinh(\theta t) + e^{-\theta^2}) \mathrm{d}t, \tag{9}$$

where $\theta=I/\sigma_n^2$. Assume that the transmission rate R_t has been calculated considering a minimum value for I, say the threshold I_T. If $I<I_T$ due to a deep fade, we have $R_t<C_{\mathrm{OOK}}$ and an outage occurs. The outage capacity is specified with respect to an outage probability P_{out}. Here,

$$P_{\mathrm{out}} = \mathrm{Prob}\{I < I_T\}. \tag{10}$$

This is equivalent to the so-called probability of fade, $P_{\mathrm{fa}}=\mathrm{Prob}(I<I_T)$ [7,32]. For the case of the LN channel model, we have [23,33]:

$$P_{\mathrm{out,LN}} = \frac{1}{2}\left[1 + \mathrm{erf}\left(\frac{\frac{1}{2}\sigma_{\ln I}^2 + \ln I_T}{\sqrt{2}\sigma_{\ln I}} \right) \right]. \tag{11}$$

For the case of the ΓΓ channel model, a closed-form expression has been developed in [34] for P_{fa}:

$$P_{\mathrm{out},\Gamma\Gamma} = \frac{\pi}{\Gamma(\alpha)\Gamma(\beta)\sin[\pi(\alpha-\beta)]} \times \left\{ \frac{(\alpha\beta)^{\beta}}{\beta\Gamma(\beta-\alpha+1)} I_T{}^{\beta}\, {}_1F_2[\beta;\beta+1,\beta-\alpha+1;\alpha\beta I_T] - \frac{(\alpha\beta)^{\alpha}}{\alpha\Gamma(\alpha-\beta+1)} I_T{}^{\alpha}\, {}_1F_2[\alpha;\alpha+1,\alpha-\beta+1;\alpha\beta I_T] \right\}. \tag{12}$$

Here, ${}_1F_2(a;c1,c2;x)$ is the generalized hypergeometric function. Note that Eqs. (11) and (12) assume high enough SNR so that the noise contribution to the received signal can be neglected.

We have presented in Fig. 8 curves of outage capacity C_{out} as a function of the receiver lens diameter D for the three turbulence cases already considered. We have set the SNR high enough that the assumption of negligible noise contribution in fading, used in the derivation of Eq. (11) and (12), can be rational. The capacity values are given conditioned to $P_{\mathrm{out}}=10^{-9}$. Setting the adequate I_T from Eq. (10), we obtain C_{out} from Eq. (9) by numerical computation. For the cases of moderate to strong turbulence, we use Eq. (12) for relatively small D. For relatively large D, the numerical computation of P_{out} becomes impossible due to values of β that are too large and thus the required numerical precision that is too high. For such values, however, we can practically make the assumption of LN distributed fading [29] and use Eq. (11) (see Subsection IV.D). For large enough D, these expressions give almost equal results.

The results of Fig. 8 confirm the previous simulation results in terms of BER. For the weak turbulence regime, the capacity is close to 1 bit per channel use even for a moderate SNR of 10 dB. For this case, a lens of about $D=20$ mm appears to be sufficiently large for approaching the maximum capacity limit in moderate to high SNR. Note that the values of C_{out} for SNR=5 dB may be too optimistic as the assumption of negligible noise variance does not really hold. For moderate to strong turbulence regimes, we have to choose $D \geq 50$ mm in order not to need a link margin that is too large. An interesting point is that for 10 mm $< D <$ 100 mm, C_{out} is smaller in the moderate turbulence regime than in the strong regime. This

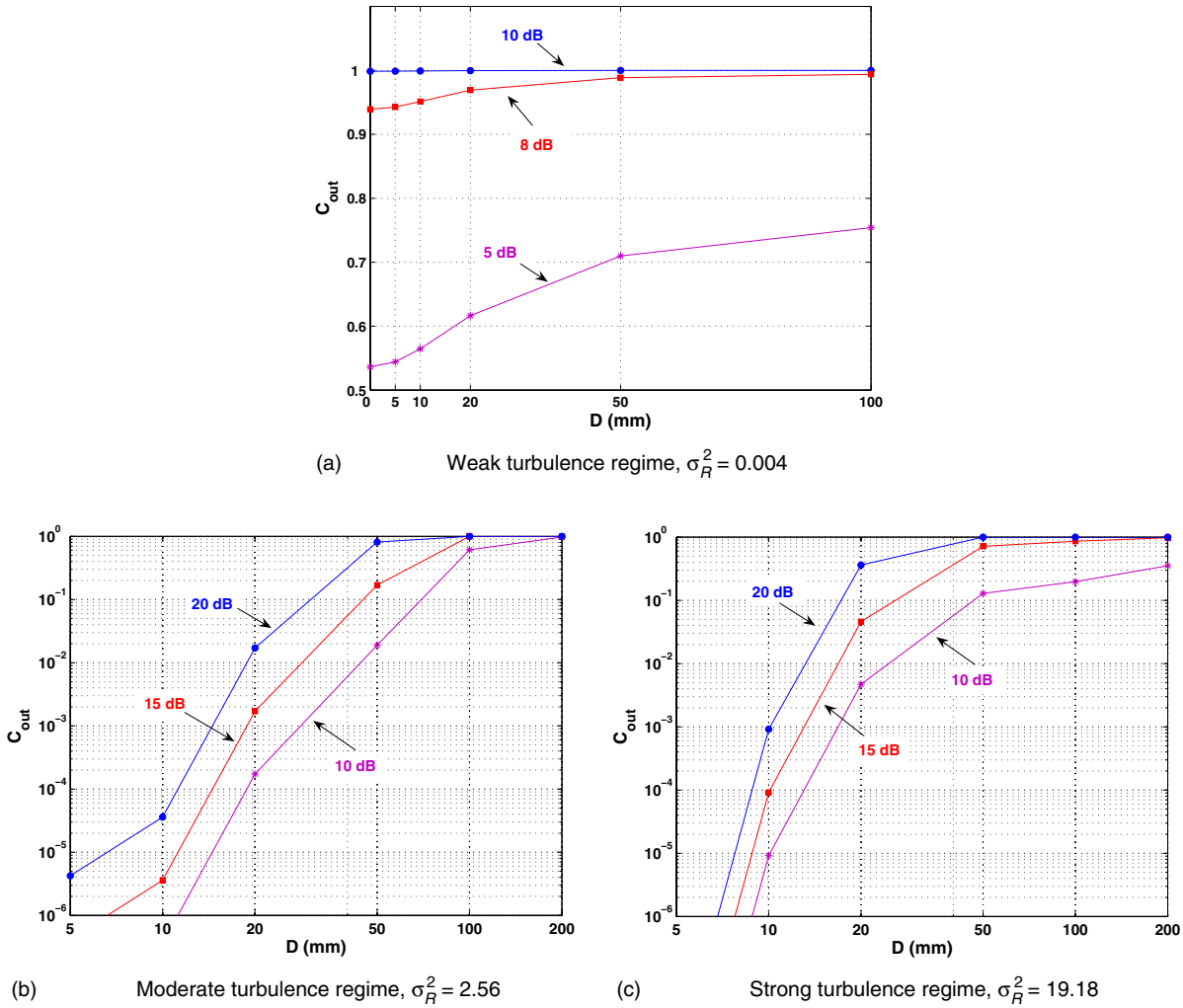

Fig. 8. (Color online) Outage capacity C_{out} (in bits per channel use) versus lens diameter D for three turbulence regimes. $P_{\text{out}}=10^{-9}$, OOK modulation, plane-wave propagation, $l_0=0$. Note that the abscissa is in linear scale for (a) and in logarithmic scale for (b) and (c).

could also be seen from the results of Figs. 3 and 4. This conclusion may be frustrating as in practice we need a larger lens for less severe turbulence. It can be explained by the fact that for $\sigma_R^2=19.18$ we are in a well-established saturation regime (concerning the scintillation index) and the scintillation speckles are widely spread at the receiver plane. For $\sigma_R^2=2.56$ we are only at the beginning of saturation and aperture averaging is less efficient.

VII. Comparison With Multiple-Aperture Systems

Efficient fading reduction can be obtained by employing spatial diversity techniques via the use of multiple beams at the transmitter [30,35] or multiple apertures at the receiver [4,8,36,37] or a combination of both [18,38–40]. Here, we consider the second technique, that is, the use of multiple lenses at the receiver, which is the simplest among the three, regarding the implementation complexity. Our aim here is to compare its efficiency with that of aperture averaging with a single lens. Compared with previous works such as [4,8], we compare the performance of single- and multiple-aperture systems in terms of BER and C_{out} without making the assumption of point receivers but by considering practical lens diameters. In addition, we make this comparison for the two cases of background- and thermal-noise-limited receivers and show the difference between them. We will see that making a choice between employing multiple apertures or a single large aperture is not straightforward and depends on the conditions of turbulence and receiver noise. Let us denote the number of receivers by M. At the receiver, we perform equal-gain combining (EGC), which provides a performance very close to that obtained by optimal combining and has the advantage of implementation simplicity [8,41].

The important point is to properly model the fade statistics for the sum of the M received signals I_{sum}. Tsiftsis *et al.* have considered in [42] the use of multiple point apertures assuming independent fading

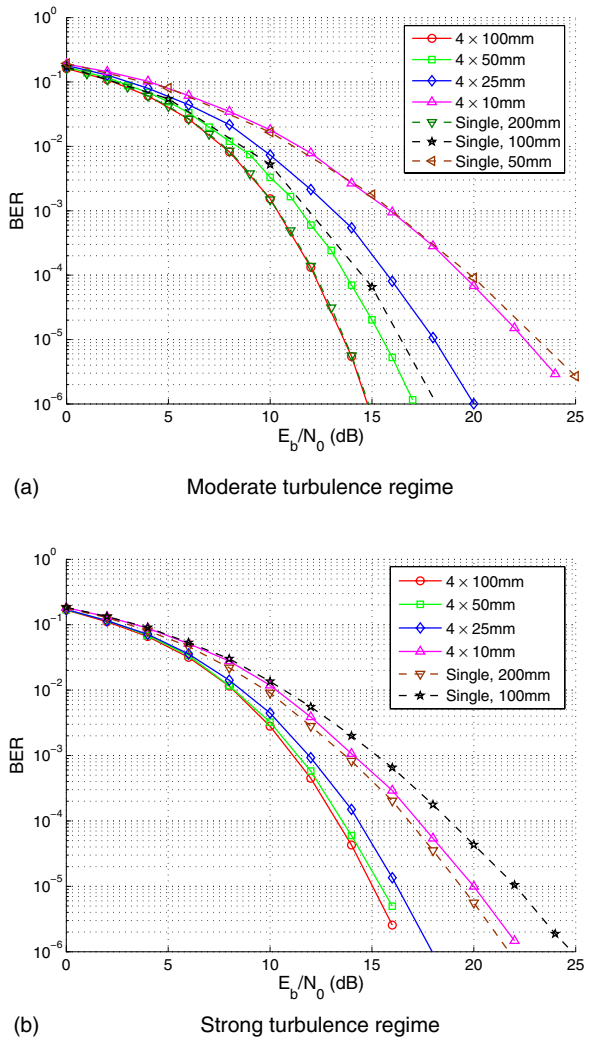

Fig. 9. (Color online) Average BER performance for multiple- and single-aperture systems for background-noise-limited receivers, OOK modulation, plane-wave propagation, $l_0=0$.

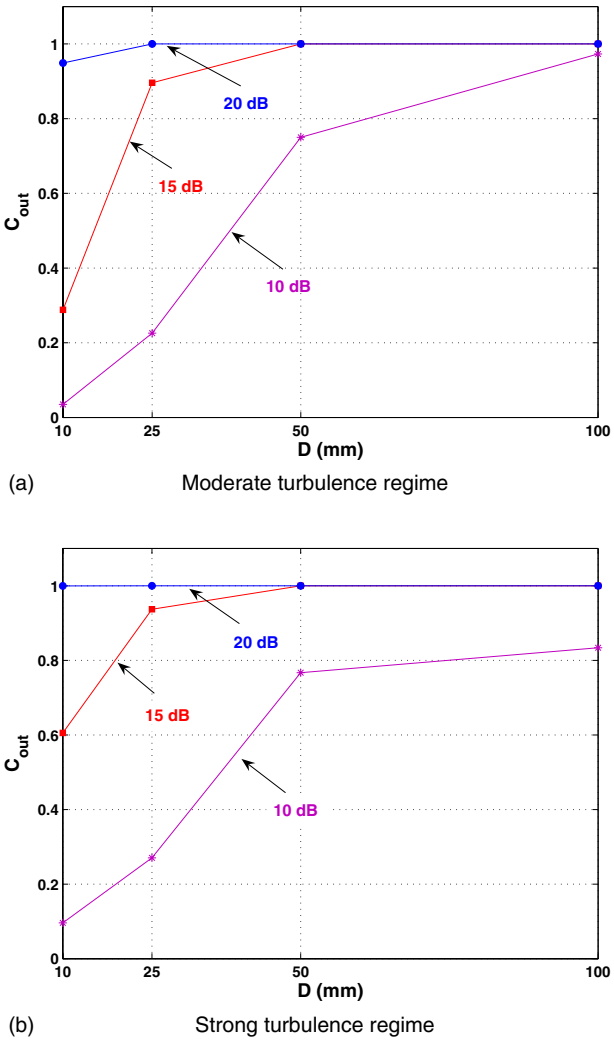

Fig. 10. (Color online) Outage capacity versus the diameter of lenses for a four-aperture receiver, $P_{out}=10^{-9}$, OOK modulation, background-noise-limited receivers, plane-wave propagation, $l_0=0$.

corresponding to different lenses. We also assume here that the pupils are separated sufficiently apart so that we have uncorrelated fading on the signals of different apertures (as it will be explained later, this is an optimistic assumption). Keeping in mind the assumptions on which the ΓΓ model is based, i.e., statistically independent large- and small-scale fluctuations I_x and I_y, and the assumption of uncorrelated fading on different receivers, I_{sum} can still be modeled by a ΓΓ distribution, with the variances of large- and small-scale fluctuations respectively given by $\sigma^2_{x,sum}=\sigma^2_{x,1}/M$ and $\sigma^2_{y,sum}=\sigma^2_{y,1}/M$, where the subscript 1 refers to one aperture. In other words, the parameters of the ΓΓ model become $\alpha_{sum}=M\alpha_1$ and $\beta_{sum}=M\beta_1$. Discussions on this modeling are provided in Subsection VII.C.

To perform a fair comparison with a single-lens aperture averaging receiver of pupil area S, we set the pupil area of each receiver for the multiple aperture case to $S_1=S/M$. In this way, we have the same received optical power for the two cases.[2] Let us consider the case of $M=4$. This is a suitable choice for a feasible geometrical design because it is considered in the *FlightStrata* product of LightPointe [43], for instance. We consider the two cases of background and thermal noise-limited receivers separately in the following.

A. Background-Noise-Limited Receivers

In this case, by increasing the pupil area by a factor m, the received signal and noise powers increase by the same factor, and hence, the SNR does not change. This was the case in all our previously presented results. We have presented in Fig. 9 the BER curves versus E_b/N_0 for the two cases of moderate and strong turbulence regimes for different lens diameter sizes.

[2]In practice, however, the overall receiver size will be larger for the multiple-aperture case due to the required lens separation to ensure low fading correlation (see Subsection VII.C).

Consider first the moderate regime in Fig. 9(a). We should compare the BER of a single aperture of diameter D with that of the multiple-aperture case with pupils of diameter $D_1=D/\sqrt{M}=D/2$. For example, if we consider a BER of 10^{-5}, the SNR gain by using four-aperture systems, compared with the corresponding single-aperture systems of diameter 50 and 100 mm, is about 5.1 and 0.92 dB, respectively. The case of four 10 mm apertures is almost as efficient as that of a single aperture of 50 mm diameter. Interestingly, we have practically the same performance for a single-aperture system of 200 mm diameter and a four-aperture system of 100 mm diameter each. We deduce that, in the moderate turbulence regime, for aperture sizes of the order of 100 mm or larger, the use of multiple apertures is not really justified. Things are different for the strong turbulence regime. As it is seen from Fig. 9(b), considering the BER of 10^{-5}, the SNR gain by using a four-aperture system compared with a single-aperture system of diameter 50 and 100 mm is about 6.63 and 4.34 dB, respectively. The gains are more considerable than what we have for the moderate regime. Interestingly, the case of four 10 mm apertures is almost as efficient as that of a single aperture of 200 mm diameter. An appropriate lens diameter for the four-aperture system would be 25 or 50 mm (for each aperture); negligible improvement is obtained by increasing the lenses' size to 100 mm.

For the sake of completeness, we have also presented the curves of outage capacity for the OOK modulation in Fig. 10. As expected, we notice a substantial increase in C_{out} for relatively small lens sizes, as compared with the single-aperture case in Fig. 8. For the lenses of diameter larger than 50 mm, the results of Fig. 10 confirm the conclusions of the previous paragraph.

B. Thermal-Noise-Limited Receivers

For thermal-noise-limited receivers, in the case of using a single lens, by increasing the pupil area, we should take into account the increase in the received power while taking the noise variance unchanged. When multiple apertures are used, however, the noise variance after EGC will be M times the noise variance for the equivalent single-aperture system. For instance, comparing a single-aperture system of 200 mm lens diameter and a four-aperture system of 100 mm lens diameter each, we have the same total received signal power, but for the latter case, the noise variance after EGC is four times larger. Let us take the case of a single-aperture system of 25 mm diameter as the reference for setting the SNRs. We have contrasted BER performances of single- and multiple-aperture systems in Fig. 11 for the case of strong turbulence [equivalent to Fig. 9(b)]. The case of a single aperture with $D=25$ mm is given just for reference. We notice that multiple-aperture systems outperform the equivalent single-aperture ones only at very low BER. In other words, at very low BER, the benefit of more diversity gain by using a multiple-aperture system overcomes the penalty of increased total receiver noise variance. As in practice we work at BERs typically of the order of 10^{-9}, the use of multiple apertures is always interesting.

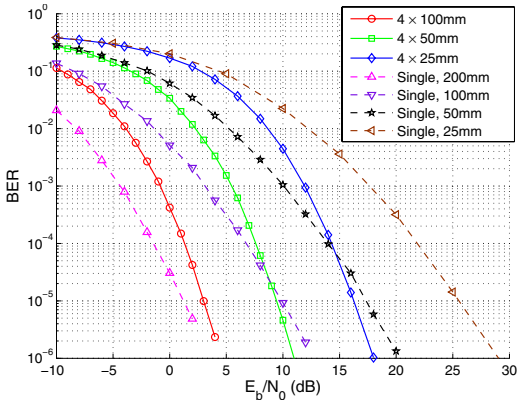

Fig. 11. (Color online) Average BER performance for multiple- and single-aperture systems for thermal-noise-limited receivers, strong turbulence regime, OOK modulation, plane-wave propagation, $l_0=0$.

C. Discussion on Fading Modeling

The maximum diversity gain is obtained for the case of uncorrelated fading on the M apertures that is valid when the lenses are spaced sufficiently apart. Notice that, if fading correlation on different apertures cannot be ignored, the results we presented should be considered as lower bounds for the BER and as upper bounds for C_{out}. However, it does not mean that using multiple pupils becomes useless in practice. For example, it is well known that for RF channels subject to Rayleigh fading and using multiple antennas at the receiver, even for correlation coefficients as large as 0.5 the fading reduction is still significant, and hence, practically interesting [44]. The effect of fading correlation on the BER performance of spatial diversity systems is studied in [45] for the case of weak turbulence.

Studying the fading correlation as a function of pupil spacing is out of the scope of this paper. Just note that the required separation to have uncorrelated fading depends not only on the link distance and beam profile but also on the turbulence strength and the lenses' size. Under weak turbulence conditions, the required spacing l_c equals the correlation length $\sqrt{\lambda L}$, which is in fact the typical size of scintillation speckles [25]. In other words, if we denote by δ the lens spacing, that is, the distance between the borders of two adjacent lenses, we should have $\delta > l_c$. For rela-

tively strong turbulence, the spatial correlation arises mainly from large-scale fluctuations, and we need larger lens spacings for reducing the fading correlation. For such a case, and assuming plane-wave propagation, we have $l_c=\lambda L/r_0$, where r_0 is the Fried parameter. In our case, given $\lambda=1550$ nm and $C_n^2=4.58\times10^{-13}$, we have $r_0=1.2$ cm and $l_c\approx6.4$ cm for the case of $L=500$ m (moderate turbulence regime) and $r_0=6.2$ mm and $l_c\approx37$ cm for the case of $L=1500$ m (strong turbulence regime). We notice that attaining the conditions of uncorrelated fading may be infeasible for the second case since the required pupil spacing is too large.

Lastly, concerning the calculation of the ΓΓ model parameters for a multiple-aperture system after EGC, note that it is suggested in [4] to use $\beta_{\text{sum}}=M\beta_1$ and $\sigma_{I,\text{sum}}^2=\sigma_{I,1}^2/M$ and to calculate α_{sum} accordingly. However, according to [30], the ΓΓ model with $\alpha_{\text{sum}}=M\alpha_1$ and $\beta_{\text{sum}}=M\beta_1$ fits better to histograms obtained from simulated data.

VIII. Conclusions and Discussions

We have studied in this paper the effect of aperture averaging on the performance of FSO systems under different conditions of turbulence and optical wave propagation. Although a part of the presented results are rather known, we brought a different perspective to the problem by considering criteria that are important from a practical point of view, such as the average bit error rate and the outage capacity. Our presented results can provide a clearer vision for evaluating the effective improvement achieved by employing aperture averaging in an FSO system. We also compared single- and multiple-aperture receivers under the conditions of background or thermal noise domination. From the presented results, we can point out the following main concluding remarks:

- For not-too-large aperture sizes, fading is more destructive for moderate turbulence than for strong turbulence conditions.
- The trade-off between link margin and outage capacity is especially important for moderate to strong turbulence conditions. Use of multiple apertures permits a substantial gain to be achieved in the outage capacity.
- Channel coding is efficient only for significantly reduced turbulence.
- The achieved performance improvement by aperture averaging is more significant for higher-order modulations like Q-ary PPM, $Q>2$.
- Use of multiple apertures is advantageous over that of a single large aperture for the strong turbulence regime, or equivalently for long-distance communication, although attaining perfect uncorrelated fading on adjacent apertures is difficult in practice. The advantage is less clear in the case of thermal-noise-limited receivers.
- For the case of moderate turbulence, employing a single large aperture would be preferable to multiple apertures, regarding the obtained performance and the receiver complexity.

Note that, in comparing single-aperture systems in terms of aperture averaging, we mostly fixed the noise variance and the average received intensity for any lens diameter D. We explained in Section II that this represents the case where background noise dominates thermal noise and when fixed FOV receivers are used. If diffraction-limited receivers are used, the amount of received background noise is essentially independent of the receiver aperture size [8,22]. In practice, for reasons of simplifying the tracking task and to alleviate beam wandering, fixed FOV receivers are used in most terrestrial FSO systems. On the other hand, if the thermal noise dominates, in addition to the fading reduction illustrated in most simulation results, by increasing D, we benefit from an SNR gain as well. The main conclusions of our work remain valid, nevertheless. We end the paper with a discussion on an important point, that is, the impact of the photodetector size.

An important assumption that we made is that we assumed a sufficiently large photodetector so that the aperture averaging is effective for any D. In fact, turbulence induces a reduction of the spatial correlation of the optical wavefront, and hence, results in an increase in the signal spatial frequency content. This, in turn, results in spreading the point-spread function at the focal plane. The aperture averaging could be less efficient if the detector area is not large enough, possibly in high rate systems, where the detector area is relatively small, and under relatively strong turbulence conditions [30]. In most FSO systems, the detector area is large enough, typically about 50 to 500 μm in diameter. When the photodetector is placed at the receiver pupil plane, no problem arises and the increase in D can result in a full benefit of aperture averaging. It is more delicate if a fiber is used to connect the pupil focal plane to the signal detection board (including the photodetector). In such a case, if a multimodal fiber is used (typically of 50 μm diameter), we are likely to still benefit fully from aperture averaging. If a monomodal fiber is used, however, as the fiber diameter is relatively small (typically 10 μm), the above-mentioned problem may arise. Note that for fiber-coupled receivers, we may have an additional loss due to poor fiber coupling resulting from a turbulence-distorted received phase of the optical beam [46]. The overall loss might be more important in multiple-aperture fiber-coupled systems as compared with a single-aperture system. This is another

criterion that may tip the balance in favor of using a single large aperture rather than several smaller apertures.

ACKNOWLEDGMENT

The authors wish to thank Frédéric Chazalet from Shaktiware Co., Marseille, France; Hassan Akhouayri and Fang Xu from Institut Fresnel, Marseille, France; and Nicolas Védrenne form ONERA, Paris, France, for their fruitful discussions. Parts of this work have been presented at the ConTEL Conference, June 2009 [29].

REFERENCES

[1] S. Bloom, E. Korevaar, J. Schuster, and H. Willebrand, "Understanding the performance of free-space optics," *J. Opt. Netw.*, vol. 2, no. 6, pp. 178–200, Jan. 2003.

[2] D. Kedar and S. Arnon, "Urban optical wireless communication networks: the main challenges and possible solutions," *IEEE Commun. Mag.*, vol. 42, no. 5, pp. 2–7, May 2004.

[3] V. W. S. Chan, "Free-space optical communications," *J. Lightwave Technol.*, vol. 24, no. 12, pp. 4750–4762, Dec. 2006.

[4] L. C. Andrews and R. L. Phillips, *Laser Beam Propagation Through Random Media*, 2nd ed. Bellingham, Washington: SPIE Press, 2005.

[5] F. Xu, M. A. Khalighi, P. Caussé, and S. Bourennane, "Channel coding and time-diversity for optical wireless links," *Opt. Express*, vol. 17, no. 2, pp. 872–887, Jan. 2009.

[6] F. Xu, M. A. Khalighi, P. Caussé, and S. Bourennane, "Performance of coded time-diversity free-space optical links," in *Queen's 24th Biennial Symp. on Communications (QSBC)*, Kingston, Canada, 2008, pp. 146–149.

[7] C. C. Davis and I. I. Smolyaninov, "The effect of atmospheric turbulence on bit-error-rate in an on-off-keyed optical wireless system," *Proc. SPIE*, vol. 4489, pp. 126–137, 2002.

[8] E. J. Lee and V. W. S. Chan, "Part 1: Optical communication over the clear turbulent atmospheric channel using diversity," *IEEE J. Sel. Areas Commun.*, vol. 22, no. 9, pp. 1896–1906, Nov. 2004.

[9] F. S. Vetelino, C. Young, L. C. Andrews, and J. Recolons, "Aperture averaging effects on the probability density of irradiance fluctuations in moderate-to-strong turbulence," *Appl. Opt.*, vol. 46, no. 11, pp. 2099–2108, Apr. 2007.

[10] J. H. Churnside, "Aperture averaging of optical scintillations in the turbulent atmosphere," *Appl. Opt.*, vol. 30, no. 15, pp. 1982–1994, May. 1991.

[11] L. C. Andrews, "Aperture-averaging factor for optical scintillations of plane and spherical waves in the atmosphere," *J. Opt. Soc. Am. A*, vol. 9, no. 4, pp. 597–600, Apr. 1992.

[12] H. Yuksel, S. Milner, and C. C. Davis, "Aperture averaging for optimizing receiver design and system performance on free-space optical communication links," *J. Opt. Netw.*, vol. 4, no. 8, pp. 462–475, Aug. 2005.

[13] L. C. Andrews, R. L. Phillips, and C. Y. Hopen, "Aperture averaging of optical scintillations: power fluctuations and the temporal spectrum," *Waves Random Media*, vol. 10, pp. 53–70, 2000.

[14] F. S. Vetelino, C. Young, and L. C. Andrews, "Fade statistics and aperture averaging for Gaussian beam waves in moderate-to-strong turbulence," *Appl. Opt.*, vol. 46, no. 18, pp. 3780–3789, June 2007.

[15] G. L. Bastin, L. C. Andrews, R. L. Phillips, R. A. Nelson, B. A. Ferrell, M. R. Borbath, D. J. Galus, P. G. Chin, W. G. Harris, J. A. Marín, G. L. Burdge, D. Wayne, and R. Pescatore, "Measurements of aperture averaging on bit-error-rate," *Proc. SPIE*, vol. 5891, no. 02, pp. 1–12, 2005.

[16] N. Perlot and D. Fritzsche, "Aperture-averaging: theory and measurements," *Proc. SPIE*, vol. 5338, pp. 233–242, 2004.

[17] L. M. Wasiczko and C. C. Davis, "Aperture averaging of optical scintillations in the atmosphere: experimental results," *Proc. SPIE*, vol. 5793, pp. 197–208, 2005.

[18] S. G. Wilson, M. B. Pearce, Q. L. Cao, and M. Baedke, "Optical repetition MIMO transmission with multipulse PPM," *IEEE J. Sel. Areas Commun.*, vol. 23, no. 9, pp. 1901–1910, Sept. 2005.

[19] H. Hemmati, *Deep Space Optical Communications*. Wiley, 2006.

[20] B. E. A. Saleh and M. C. Teich, *Fundamentals of Photonics*. Wiley, 1991.

[21] X. Zhu and J. M. Kahn, "Pilot-symbol assisted modulation for correlated turbulent free-space optical channels," *Proc. SPIE*, vol. 4489, pp. 138–145, 2002.

[22] R. M. Gagliardi and S. Karp, *Optical Communications*, 2nd ed. Wiley, 1995.

[23] L. C. Andrews, R. L. Phillips, and C. Y. Hopen, *Laser Beam Scintillation with Applications*. Bellingham, Washington: SPIE Press, 2001.

[24] A. K. Majumdar and J. C. Ricklin, *Free-Space Laser Communications: Principles and Advances*. Springer-Verlag, 2007.

[25] S. Bloom, "The physics of free-space optics," AirFiber Inc., White Paper, May 2002.

[26] D. L. Fried, "Optical resolution through a randomly inhomogeneous medium for very long and very short exposures," *J. Opt. Soc. Am.*, vol. 56, no. 10, pp. 1372–1379, Oct. 1966.

[27] A. Consortini, E. Cochetti, J. H. Churnside, and R. J. Hill, "Inner-scale effect on irradiance variance measured for weak-to-strong atmospheric scintillation," *J. Opt. Soc. Am. A*, vol. 10, no. 11, pp. 2354–2362, Nov. 1993.

[28] J. M. Martin and S. M. Flatté, "Intensity images and statistics from numerical simulation of wave propagation in 3-D random media," *Appl. Opt.*, vol. 27, no. 11, pp. 2111–2126, June 1988.

[29] M. A. Khalighi, N. Aitamer, N. Schwartz, and S. Bourennane, "Turbulence mitigation by aperture averaging in wireless optical systems," *Proc. of ConTEL Conf.*, Zagreb, Croatia, 2008, pp. 59–66.

[30] J. A. Anguita, M. A. Neifeld, and B. V. Vasic, "Spatial correlation and irradiance statistics in a multiple-beam terrestrial free-space optical communication link," *Appl. Opt.*, vol. 46, no. 26, pp. 6561–6571, Sept. 2007.

[31] F. Dios, J. Recolons, A. Rodriguez, and O. Batet, "Temporal analysis of laser beam propagation in the atmosphere using computer-generated long phase screens," *Opt. Express*, vol. 16, no. 3, pp. 2206–2220, Feb. 2008.

[32] J. L. Massey, "Capacity, cutoff rate, and coding for a direct-detection optical channel," *IEEE Trans. Commun.*, vol. 29, no. 11, pp. 1651–1621, Nov. 1981.

[33] H. T. Yura and W. G. McKinley, "Optical scintillation statistics for IR ground-to-space laser communication systems," *Appl. Opt.*, vol. 22, no. 21, pp. 3353–3358, Nov. 1983.

[34] M. A. Al-Habash, L. C. Andrews, and R. L. Philips, "Mathematical model for the irradiance probability density function of a laser beam propatating through turbulent media," *Opt. Eng.*, vol. 40, no. 8, pp. 1554–1562, Aug. 2001.

[35] P. Polynkin, A. Peleg, L. Klein, T. Rhoadarmer, and J. Moloney, "Optimized multiemitter beams for free-space optical communications through turbulent atmosphere," *Opt. Lett.*, vol. 32, no. 8, pp. 885–887, Apr. 2007.

[36] E. J. Lee and V. W. S. Chan, "Diversity coherent receivers for optical communication over the clear turbulent atmosphere," *IEEE Int. Conf. Communications*, 2007, pp. 2485–2492.

[37] M. Razavi and J. H. Shapiro, "Wireless optical communications via diversity reception and optical preamplification," *IEEE Trans. Wireless Commun.*, vol. 4, no. 3, pp. 975–983, May 2005.

[38] D. C. O'Brien, S. Quasem, S. Zikic, and G. E. Faulkner, "Multiple input multiple output systems for optical wireless: challenges and possibilities," *Proc. SPIE*, vol. 6304, pp. 16-1–16-7, 2006.
[39] D. Bushuev and S. Arnon, "Analysis of the performance of a wireless optical multi-input to multi-output communication system," *J. Opt. Soc. Am. A*, vol. 23, no. 7, pp. 1722–1730, July 2006.
[40] S. Hranilovic, *Wireless Optical Communication Systems*. Springer-Verlag, 2005.
[41] M. A. Khalighi, K. Raoof, and G. Jourdain, "Capacity of wireless communication systems employing antenna arrays, a tutorial study," *Wireless Personal Communications*, vol. 23, no. 3, paper 321352, Dec. 2002.
[42] T. A. Tsiftsis, H. G. Sandalidis, G. K. Karagiannidis, and M. Uysal, "Optical wireless links with spatial diversity over strong atmospheric turbulence channels," *IEEE Trans. Wireless Commun.*, vol. 8, no. 2, pp. 951–957, Feb. 2009.
[43] "Design concepts of the FlightStrata optical wireless system with beam tracking and automatic power control," LightPointe, White Paper, 2004, http://www.lightpointe.com.
[44] J. Salz and J. H. Winters, "Effect of fading correlation on adaptive arrays in digital mobile communication systems," *IEEE Trans. Veh. Technol.*, vol. 43, no. 4, pp. 1049–1057, Nov. 1994.
[45] S. M. Navidpour, M. Uysal, and M. Kavehrad, "BER performance of free-space optical transmission with spatial diversity," *IEEE Trans. Wireless Commun.*, vol. 6, no. 8, pp. 2813–2819, Aug. 2007.
[46] C. Ruilier and F. Cassaing, "Coupling of large telescopes and single-mode waveguides: application to stellar interferometry," *J. Opt. Soc. Am. A*, vol. 18, no. 1, pp. 143–149, Jan. 2001.

Mohammad-Ali Khalighi (M'99, SM'07) received his B.Sc. and M.Sc. degrees in electrical engineering from Sharif University of Technology, Tehran, Iran, in 1995 and 1997, respectively, and his Ph.D. in electrical engineering (telecommunications) from the Institut National Polytechnique de Grenoble (INPG), France, in 2002. From 2002 to 2005, he has been with GIPSA-lab, Télécom Paris-Tech (ENST), and IETR-lab, as a Postdoctoral Research Fellow. He joined École Centrale Marseille and Institut Fresnel in 2005 as an Assistant Professor. His main research interests include coding, signal detection, and channel estimation for wireless communication systems.

Noah Schwartz received his M.Sc. in engineering from the University of Nice Sophia-Antipolis, France, in 2005. From 2005 to 2006, he worked at the observatory of Paris-Meudon. He is currently working toward his Ph.D. in physics at the Department of High Angular Resolution at ONERA. His current research interests include adaptive optics, atmospheric turbulence, laser beam control, and free-space optical communications.

Salah Bourennane received his Ph.D. degree from the Institut National Polytechnique de Grenoble (INPG), France, in 1990 in signal processing. Currently, he is a Full Professor at École Centrale Marseille, and he is the head of the Multidimensional Signal Processing team at Institut Fresnel, Marseille, France. His research interests include statistical signal processing, array processing, image processing, multidimensional signal processing, and telecommunications.